

The Wolf-Rayet features and mass-metallicity relation of long-duration gamma-ray burst host galaxies

X. H. Han^{1,2,3,4*}, F. Hammer^{2**}, Y. C. Liang³, H. Flores², M. Rodrigues², J. L. Hou¹, J. Y. Wei³

¹ Key Laboratory for Research in Galaxies and Cosmology, Shanghai Astronomical Observatory, the Chinese Academy of Sciences, 80 Nandan Road, Shanghai, 200030, China

² GEPI, Observatoire de Paris-Meudon, Meudon 92195, France

³ National Astronomical Observatories, Chinese Academy of Sciences, Beijing 100012, China

⁴ Graduate School of the Chinese Academy of Sciences, Beijing 100049, China

Received ; accepted

ABSTRACT

Aims. We have gathered optical spectra of 8 long-duration GRB host galaxies selected from the archival data of VLT/FORS2. We investigated whether or not Wolf-Rayet (WR) stars can be detected in these GRB host galaxies. We also tried to estimate the physical properties of GRB host galaxies, such as metallicity.

Methods. We identified the WR features in these spectra by fitting the WR bumps and WR emission lines in blue and red bumps. We also identified the subtypes of the WR stars, and estimated the numbers of stars in each subtype, then calculated the WR/O star ratios. The (O/H) abundances of GRB hosts were estimated from both the electron temperature (T_e) and the metallicity-sensitive strong-line ratio (R_{23}), for which we have broken the R_{23} degeneracy. We compared the environments of long-duration GRB host galaxies with those of other galaxies in terms of their luminosity (stellar mass)-metallicity relations ($L - Z$, $M_* - Z$).

Results. We detected the presence of WR stars in 5 GRB host galaxies having spectra with relatively high signal-to-noise ratios (S/N). In the comparison of $L - Z$, $M_* - Z$ relations, it shows that GRB hosts have lower metallicities than other samples with comparable luminosity and stellar mass. The presence of WR stars and the observed high WR/O star ratio, together with low metallicity, support the “core-collapsar” model and implicate the first stage of star formation in the hosted regions of GRBs.

Key words. Gamma rays: bursts - Stars: Wolf-Rayet - Galaxies: abundances - Galaxies: fundamental parameters

1. Introduction

Gamma ray bursts (GRBs), the most energetic events in the Universe, were discovered accidentally in the 1960s (Klebesadel, Strong & Olson 1973). Since then, GRBs have been the targets of intense researches. However, the mechanism of bursts and the identity of progenitors of GRBs are still under discussion.

The durations of GRBs, together with their spectral properties, suggest a classification of short (with duration ≤ 2 s and hard spectrum) and long bursts (with duration ≥ 2 s and soft spectrum) (Kouveliotou et al. 1993; Hartmann 2005). Short GRBs are believed to originate from the merger of compact binaries: double neutron star binaries (NS-NS); black hole - neutron star binaries (BH-NS), for example. For long GRBs, the favored “core-collapsar” model starts from the idea of a rapidly rotating, massive star that has undergone extreme gravitational collapse and formed a central black hole (Woosley et al. 1993; MacFadyen & Woosley 1999; Klose et al. 2004). According to the collapsar model, the prompt energetic structure of a long GRB is the result of energy dissipation by internal, relativistic shocks, which may last seconds or minutes, at a radius of about 10^{14} cm from the center of the collapsed star (Hartmann 2005 and references therein). Moreover, the association between GRBs and supernovae (SNe) indicates that in many cases the parent SN population of GRBs is formed by peculiar type Ibc SNe.

Wolf-Rayet (WR) stars are naturally considered to be the most favored candidates of long duration GRB progenitors. In the stellar evolution model of Hirschi et al. (2005), WR stars, the massive short lived stars, satisfy the main criteria for GRBs production (black hole formation, loss of hydrogen-rich envelope, and enough angular momentum to form an accretion disk around the black hole). According to this model, a lower limited metallicity interval at subsolar values (typically at Z_{SMC} to Z_{LMC} , i.e. $Z \sim 0.2$ - $0.4 Z_{\odot}$) is also a criterion of GRB production. However, magnetic fields breaking poses some difficulties to produce GRBs (Petrovic et al. 2005). To solve this problem, one possible scenario is assuming that the star at the lower metallicity is rotating so fast that mixing takes place and the star evolves chemically homogeneously, so it does not have the hydrogen envelope. Moreover, that lower metallicity (typically $Z \leq 0.05 Z_{\odot}$) leads to a low mass loss and therefore keeps a high angular momentum. Those conditions are necessary to produce a GRB (Woosley & Heger 2006; Yoon & Langer 2005). Therefore, it is imperative to confirm the presence of WR stars and to better determine metallicities in the region of GRBs.

The subtype and number of WR stars, together with the relative WR/O star number ratio, are connected with the star-forming activity and the star burst duration in galaxies. We can gain a greater understanding of the evolutionary paths of long-duration GRB progenitors by detecting WR populations within GRB host galaxies. Moreover, the evolutionary model suggests that metallicity, one of the important indicators for the evolution history of galaxies, affects the properties of WR stars (Schaerer & Vacca 1998). Crowther & Hadfield (2006) investigated the

* email: hxx@nao.cas.cn

** email: francois.hammer@obspm.fr

effect of metallicity on luminosities of WR lines. They found reduced WR line luminosities at low metallicity, which means there is a lower WR/O star ratio with decreasing metallicity. However, the high WR/O star ratios are found in GRB 980425 and GRB 020903 host galaxies, which have low metallicities (Hammer et al. 2006). The WR/O star ratio - metallicity relation for other GRBs is still unknown.

The first detection of a counterpart of a GRB at optical and X-ray was done on 28 February 1997 (van Paradijs et al. 1997). Since the discovery of GRB afterglows, the GRB host galaxies and their redshifts could be identified. From 1997 to 2007, 588 GRBs have been detected. Among them, 325 GRBs had X-ray afterglows, 220 GRBs had optical afterglows and 55 GRBs had radio afterglows¹.

The study of GRB host galaxies is very important for understanding the physical properties of GRB regions and the nature of GRB progenitors. Although a large number of host galaxies can be identified, most of them are too faint to be observed even using the biggest telescopes in the world. So far, only a few dozens of host galaxies have been spectroscopically observed (e.g. **GHostS**). Moreover, the number of GRB hosts, which have been intensively spectroscopically studied, is even less.

Evidence from photometric and spectroscopic observations shows that the host galaxies of long-duration GRBs are mostly faint, blue, low-mass, star-forming galaxies with low metallicities (Sokolov et al. 2001; Le Floch et al. 2003; Fynbo et al. 2003; Courty et al. 2004; Prochaska et al. 2004; Christensen et al. 2004; Chary et al. 2002; Gorosabel et al. 2005; Fynbo et al. 2006; Wiersema et al. 2007; Kewley et al. 2007; Savaglio, et al. 2009, hereafter Savaglio09; Levesque et al. 2009). On the contrary, the host galaxies of short-duration GRBs mostly have higher luminosities and higher metallicities than long-duration GRB hosts (Berger 2008).

We study a sample of 8 long-duration GRB hosts with good spectroscopic observations. Firstly, we try to detect the WR features in these GRB hosts, then to study the physical properties of GRB host galaxies, such as their metallicities and luminosity (stellar mass)-metallicity relations ($L - Z$, $M_* - Z$). This paper is organized as follows. The sample selection and flux measurements are performed in Sect. 2. In Sect. 3, we describe the identification of the WR features in spectra of GRB hosts. In Sect. 4, the physical properties of GRB host galaxies are discussed. The discussion and conclusion are presented in Sect. 5. Throughout the paper, we adopt the Λ CDM cosmological model ($H_0 = 70$ km s⁻¹ Mpc⁻¹, $\Omega_M = 0.3$ and $\Omega_\Lambda = 0.7$), and the initial mass function (IMF) proposed by Salpeter (1955). All the comparisons used in this work are normalized by the same Λ CDM cosmological model and IMF. All the magnitudes in this paper are in the Vega system.

2. Data reduction and measurements

2.1. The sample selection and data reduction

One of the main goals of this work is to find evidence of the presence of WR stars in GRB hosts through optical spectroscopic analysis. We investigated archival data from VLT/FORS2² to get the spectra of GRB host galaxies with $z < 1$, which ensures enough emission lines are included in the spectral coverage. These spectra taken with 600B, 600RI, 600Z grisms ($R \sim$

1300), and 300V grism ($R \sim 400$) of FORS2 were adopted, because of their good compromise between relatively high spectral resolution, which allows to resolve the WR features, and relatively high sensitivity, which supplies spectra with high quality.

Data reduction and extraction were performed using a set of IRAF³ procedures developed by our team, which can simultaneously reconstruct the spectra and the sky counts of the objects. For some GRBs associated with supernovae, the early-time spectra have been checked carefully to avoid the contamination of supernovae, which makes WR features hard to be identified and increases the error of emission line flux. Then spectra having contaminations of supernovae were removed.

Wavelength calibration was performed using the HeNeAr lamp spectra. Flux calibration was achieved by observing spectrophotometric stars with the same grism and the same slit width. Galactic extinction was adopted from NED⁴, Schlegel et al. (1998). All spectra have been transformed into the rest-frame. The spectra taken with different grism, but the same resolution and the same slit width were merged to widen the wavelength coverages (e.g. GRB 980703; GRB 020903). When merging spectra, the exposure times were applied as weighting. The sample has 8 objects including 7 long-duration GRB hosts and 1 possible long-duration GRB host (GRB 060505). The host of GRB 060505 was spatially resolved by VLT/FORS2 spectroscopic observations, therefore the GRB region and the entire host galaxy were studied, separately (see Thöne et al. 2008 for the imaging). The detailed discussion about GRB 060505 is given in Sect. 5.

Table 1 lists those 8 GRB hosts in our sample with the name, coordinate at 2000 epoch, redshift, and burst type. The detailed observational information (date, exposure time, seeing, grism, and program) for the objects is given in Table 2.

2.2. Flux measurements of emission lines

In order to measure the accurate emission line fluxes, the continuum and absorption lines should be subtracted from the spectrum carefully. To do this, the STARLIGHT⁵, a spectral synthesis code, developed by Cid Fernandes et al. (2005), is used to fit the observed spectrum. STARLIGHT can model the continuum and stellar absorption lines using a linear combination of N_* simple stellar populations (SSP) templates from the evolutionary population synthesis code of Bruzual & Charlot (2003). In the fitting, we use a base of 45 SSPs, which includes 15 ages (0.001, 0.003, 0.005, 0.01, 0.025, 0.04, 0.1, 0.28, 0.64, 0.9, 1.4, 2.5, 5, 10, 13 Gyr) at 3 metallicities (0.2, 1, 2.5 Z_\odot). Galactic extinction law of Cardelli et al. (1989) (CCM) was adopted in the STARLIGHT fitting. An example of spectral fitting is shown in Figure 1.

Emission line fluxes were measured manually using SPLOT task in IRAF. The errors are mainly from three sources: the first one is the uncertainty from the fitting of the continuum and stellar absorption line; the second one is the uncertainty in flux measurement; the third one is the Poisson noises from both sky and objects, and actually dominate the error budgets. Emission line fluxes corrected for Galactic extinction are given in Table 3.

¹ For the most complete list of GRBs, see the URL: <http://www.mpe.mpg.de/~jcg/grbgen.html>, maintained by J. Greiner.

² <http://archive.eso.org/eso/eso-archive-main.html>

³ IRAF is distributed by the National Optical Astronomical Observatories, and is operated by the Association of Universities for Research in Astronomy, Inc., under cooperative agreement with the National Science Foundation.

⁴ <http://nedwww.ipac.caltech.edu/>

⁵ <http://www.starlight.ufsc.br>

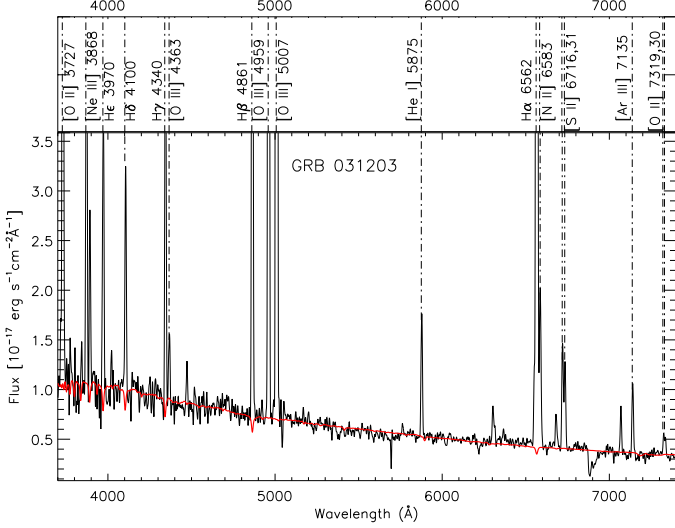


Fig. 1 The spectrum of GRB 031203 host galaxy. The spectral synthesis fitting is plotted in red line. The strong emission lines are marked.

2.3. Dust extinction

The dust extinction can be estimated from the Balmer-line ratios ($H\alpha/H\beta$, $H\gamma/H\beta$, and $H\alpha/H\gamma$). Case B recombination with an electron density of 100 cm^{-3} and a temperature of $10\,000 \text{ K}$ was adopted in the dust extinction calculation. The predicted intrinsic ratio is 2.86 for $I_0(H\alpha)/I_0(H\beta)$, and 0.466 for $I_0(H\gamma)/I_0(H\beta)$ (Osterbrock 1989). We applied the Galactic extinction law of CCM with $R_V = 3.1$ as the ratio of A_V to $E(B-V)$ (Seaton 1979). The values of dust extinction are listed in Table 4. The 2 extinction values of each object derived from the ratios of $H\alpha/H\beta$ and $H\gamma/H\beta$ are consistent. The $E(B-V)$ derived from $H\alpha/H\beta$ is adopted in this study when available, because the higher S/N ratios of these two lines can ensure the higher accuracies of the results. The $E(B-V)$ derived from $H\gamma/H\beta$ is adopted for GRB 980703 and 020405, because $H\alpha$ is not available in their spectra. Then we corrected emission line fluxes for dust extinction.

3. Wolf-Rayet bump identification

The main WR features often seen in optical spectra of galaxies are two characteristic broad emission line clusters. One is in the blue part of the spectrum at around $4600\text{--}4680 \text{ Å}$ (hereafter blue bump, Allen et al. 1976; Kunth & Joubert 1985; Conti 1991; Schaerer & Vacca 1998). The other one is in the red region around $5650\text{--}5800 \text{ Å}$ (hereafter red bump, Kunth & Schild 1986; Dinerstein & Shields 1986). The blue bump is actually a blend of some broad WR lines, such as N V 4605, 4620 Å, N III 4634, 4640 Å, C III/C IV 4650, 4658 Å and He II 4686 Å, and some nebular emission lines superposed on the bump, such as [Fe III] 4658 Å, He II 4686 Å, He I + [Ar IV] 4711 Å and [Ar IV] 4740 (Guseva et al. 2000; Izotov et al. 1998). The red bump is usually much weaker than the blue bump. C IV 5808 Å is commonly seen in the red bump (Kunth & Schild 1986; Dinerstein & Shields 1986).

The number of WR stars can be estimated from the luminosity of the blue and red bumps divided by the luminosity of a single WR star in a certain subtype (see, e.g. Guseva et al. 2000). In the following three subsections, we firstly try to identify the WR

features in our GRB hosts, and then try to estimate the subtypes and numbers of WR stars, and finally summarize the results of these GRB host galaxies.

3.1. Identifying the WR features

To identify the WR features, we select the spectra of GRB hosts with good quality. The criterium for this selection is assumed to be $S/N > 10$ in continuum on both sides of the blue bump to ensure that the WR features detected are real and that a final-selected sample is as large as possible. For other cases, there are very few chances to identify the WR features, even if they do actually exist in the spectra. This final-selected sample includes 5 objects: GRB 980703, GRB 020405, GRB 020903, GRB 031203, GRB 060218.

We identify the WR features for these 5 GRB hosts based on the appearance of the blue bump and WR emission lines by fitting them. This fitting method is also used by Brinchmann et al. (2008) (hereafter B08). The fitting is performed using the SPECFIT routine in IRAF. We fit the whole blue bump with a single broad gaussian profile. To fit the WR lines N V 4605, 4620 Å, N III 4640 Å, C III/C IV 4650, 4658 Å and He II 4686 Å, when they exist, we adopt multiple gaussian profiles to distinguish the broad component, which is mainly from WR stars, from the narrow component, which is mainly from nebulae. Nebular lines, blended in the bump, are also fitted. The $FWHMs$ of narrow components of WR lines are set to be consistent with those of nebular lines. When carrying out the fit, the best-fit continuum is chosen very carefully, because the WR features depend sensitively on the continuum estimates. We limit the overall wavelength shift of the blue and red features to be $|\Delta\lambda| \leq 3 \text{ Å}$ and the width of the broad component of WR lines to be $\sim 3000 \text{ km s}^{-1}$ $FWHM$, which are reasonable values found by B08. The fluxes of WR bumps and WR lines are measured from the fitted spectra. The fits are shown in Figure 2. A significant He I 5875 Å, evidence of the presence of young stars such as WR stars, is detected in all the 5 objects.

3.2. Identifying the subtypes of WR stars and estimating their numbers

The WR features in galaxies are mainly contributed from two types of WR stars (WN, WC). In the WN types, the emission lines from helium and nitrogen ions are often seen in the spectra. The emission lines from helium, carbon and oxygen can be considered as the features of WC types. The relative strengths of these emission lines determine the early (E) and late (L) subtypes of WN stars (WNE, WNL) (e.g., van der Hucht et al. 1981; Conti et al. 1983; Vacca & Conti 1992), and WC stars (WCE, WCL) (e.g., Torres et al. 1986; Vacca & Conti 1992). In the blue bump, the broad WR emission lines, such as N V 4605, 4620 Å, N III 4634, 4640 Å, C III/C IV 4650, 4658 Å, He II 4686 Å are mainly produced by WNL and WCE stars. In the red bump, C IV 5808 Å is emitted by WCE. Normally, WNE stars cannot be distinguished from other WR stars, since they can emit all these lines. However their contribution to the bump can be ignored because of their lower luminosity and shorter lifetime compared with those of WNL. WCL stars can be identified by C III 4650, 5696 Å emission lines. There is another type of WR star, WO, which can be identified by the presence of oxygen lines. Subtypes of WO stars can be classified according to the relative strengths of their oxygen lines (Barlow & Hummer

1982; Vacca & Conti 1992). Among our sample, none of them shows the features of WO stars.

The number of WR stars in a certain subtype can be estimated from the total luminosity of the blue and/or red bumps divided by the luminosity of a single WR star (Guseva et al. 2000). To get the accurate luminosities of the bumps, the contributions from nebular lines should be subtracted from the bumps.

The number of WCE stars can be derived directly from luminosity of the red bump, since that luminosity is only contributed by WCE stars. Usually, WCE stars are represented by WC4 stars. According to the evolutionary synthesis model for WR stars presented by Schaerer & Vacca (1998), the luminosity of a single WC4 star is 3.0×10^{36} ergs s^{-1} in the red bump.

To determine the number of WNL stars, we use the luminosity of the blue bump subtracted by the contribution of WCE stars. The contribution of WCE in the blue bump can be estimated from the ratio between the luminosity of WC4 stars in the red bump and that in the blue bump,

$$k = \frac{L_{WC4}(\lambda 4658)}{L_{WC4}(\lambda 5808)}. \quad (1)$$

Several values of coefficient k were given by previous works. We adopted the value of $k = 1.71 \pm 0.53$ given by Schaerer & Vacca (1998). Usually, WNL stars are represented by WN7 stars. The luminosity of a single WN7 in the blue bump, which depends on the metallicity, is 2.0×10^{36} ergs s^{-1} for $Z < Z_{\odot}$, or 2.6×10^{36} ergs s^{-1} for $Z > Z_{\odot}$ (Schaerer & Vacca 1998). The first one is adopted in this work, since our samples basically have lower metallicity than solar (see Sect. 4).

The number of WCL stars can be estimated from the luminosity of C III 5696 Å. For a WCL single star, the value of luminosity of C III 5696 Å adopted in this work is 8.1×10^{36} ergs s^{-1} (Schaerer & Vacca 1998, Guseva et al. 2000). However, the luminosity of this weak line in a single star is still not well known.

The ratio of relative WR/O star number can be estimated by two methods from optical spectra. The method developed by Arnault et al. (1989) uses the flux in the entire WR blue bump, while another one (Vacca & Conti 1992) only uses the flux of the broad He II 4686 Å line. We use the first one in this work, since it is more suitable for low resolution spectra, for which the broad He II 4686 Å line cannot be separated clearly from the bump. The formula is

$$\log \left[\frac{WR}{(WR + O)} \right] = (-0.11 \pm 0.02) + (0.85 \pm 0.02) \log \left(\frac{L_{blue\ bump}}{L_{H\beta}} \right). \quad (2)$$

For each GRB host, fluxes and luminosities of WR bumps and weak WR features are given in Table 5. Note that fluxes given here are not corrected for the interstellar extinction, while luminosities are absolute ones, which are transformed from these fluxes after being corrected for the extinction.

Several sources contribute to the uncertainties of estimating the numbers of WR stars. Besides the effects of k and the luminosity of a single WN star, there are three other sources, such as the observational uncertainty, the errors of multi-component profile fit and the contamination from nebular lines to the blue bump. They could lead to an uncertainty, assumed to be 30 - 60 %, for the number of WR stars and the WR/O star number ratio.

3.3. The results

We present the WR features and the numbers of WR stars of each of our GRB hosts in detail as follows, which are also given in Table 5.

GRB 980703 - The S/N in continuum on both sides of the blue bump (hereafter S/N*) is about 12. We do not detect the convincing WR bump in the spectrum. However, two WR lines, C IV 4658 Å and He II 4686 Å are identified. They can be emitted by WNL and WCE stars (Schaerer & Vacca 1998; B08). The red bump is not included in the spectral coverage. Therefore, we cannot verify WR star subtypes.

GRB 020405 - The S/N* is 10. A blue bump can be seen clearly in the spectrum. Some broad WR lines, N II 4640 Å, C III 4650 Å, C IV 4658 Å and He II 4686 Å are identified in the bump, which implies the presence of WNL and WCE. The weak C III 4650 Å indicates the presence of WCL stars. The WR subtypes and the number of WR stars cannot be verified since there is no red part of the spectrum.

GRB 020903 - The S/N* is about 16. A strong blue bump is detected in the spectrum. Broad lines N V 4605, 4620 Å, C IV 4658 Å, and C IV 5808 Å indicate the existence of WNL and WCE stars (B08). The number of WCE stars is estimated by using the luminosity of the red bump, which can be interpreted as produced by 1070 ± 210 WCE stars. Adopting the value of $k = 1.71 \pm 0.53$, the contribution of these WCE stars in the blue bump is $5.49 \pm 1.81 \times 10^{39}$ erg s^{-1} . After subtracting the contribution of WCE stars, the luminosity of WNL stars in the blue bump is $4.23 \pm 1.46 \times 10^{39}$ erg s^{-1} , which corresponds to 2117 ± 721 WNL stars.

GRB 031203 - The S/N* is about 20. The strong signature of the blue bump is shown in the spectrum. The broad WR lines C IV 4658 Å, He II 4686 Å are detected in the blue bump. In the red part, we do not detect the characteristic line of WCE, C IV 5808, which implies that the number of WCE in this galaxy can be ignored. Besides that, the other two WR lines, N III 4905 Å, N II 5720-40 are also detected. All these WR features suggest the presence of WNL stars (Smith et al. 1996; Guseva et al. 2000; B08). The number of WNL stars is 1585 ± 540 which is estimated from the luminosity of the blue bump.

GRB 060218 - The S/N* is higher than 40. Many WR lines are identified, including N III 4512 Å, N V 4620 Å, N II 4640 Å, He II 4686 Å, He I/N II 5047 Å and N II 5720-40 Å. All these lines show the characteristics of WNL stars (Massey & Conti 1980, 1983; Crowther & Smith 1997; Guseva et al. 2000; B08). Two WR lines, C III 4650 Å, and C II 5696 Å are also identified, which are the characteristics of the WCL stars (B08). The presence of WCE stars cannot be confirmed, since no C IV 5808 is detected. Using the luminosity of the blue bump, we estimate the number of WNL stars to be 324 ± 120 . The luminosity of C III 5696 Å corresponds to 31 ± 10 WCL stars.

The relative WR/O star number ratios are estimated using the luminosities of blue bumps and H β . For the hosts of GRB 020405, 020903, 031203 and 060218, the ratios are 0.26 ± 0.08 , 0.21 ± 0.06 , 0.09 ± 0.02 and 0.11 ± 0.04 , respectively.

In summary, obvious WR features are detected in 4 spectra out of 5 long-duration GRB hosts, except for GRB 980703 that shows no convincing WR bump but two WR lines. Moreover, the numbers of WR stars for 3 GRB hosts are in a range from 300 to 6000, which is consistent with the typical number of WR stars ($\sim 100 - 10^5$, Vacca & Conti 1992; Guseva et al. 2000) in WR galaxies. Also, high WR/O star number ratios are estimated in these 4 GRB hosts. Therefore, the presence of WR stars in these GRB hosts is verified. However, since the small sample here, the conclusion that WR stars exist in all the long-duration GRB hosts still cannot be made strongly. Anyway, the results of this work show positive evidence of the scenario that WR stars

are the progenitors of long GRBs. These are consistent with the previous studies below.

Hammer et al. (2006) have firstly discovered the presence of WR stars in three nearby long-duration GRB host galaxies (GRB 980425, GRB 020903, GRB 031203) from deep spectroscopic observations. Since then, few works have been done to detect WR features in long-duration GRB hosts. Margutti et al. (2007) claimed that the identification of WR emission lines in GRB 031203 is uncertain. However, their Figure 3 does show the strong WR blue bump. The N III 4640 Å and C IV 4658 Å blended broad lines can also be identified in the bump, which was not attempted in their work. Wiersema et al. (2007) did not detect the obvious He II 4686 Å and WR bump in GRB 060218. However, we notice that the UVES spectra they used were taken at the time close to the burst, which means the significant contamination from the associated SN 2006aj cannot be ignored in the WR feature identification. In their work, an upper limit of WR/(WR + O) stars is estimated to be < 0.4 , which is consistent with the result ($\text{WR/O} = 0.11 \pm 0.04$) estimated in this work.

4. The physical properties of GRB host galaxies

Metallicity is a fundamental parameter to probe into the properties of GRB progenitors and the environment of GRB regions. Strong emission lines in spectra of GRB host galaxies allow us to estimate metallicities. The luminosity (stellar mass)–metallicity ($L - Z$, $M_* - Z$) relation of galaxies is a fundamental relation to show their evolutionary status and star-formation histories. We estimate the metallicities of these GRB hosts, and then study them in terms of the $L - Z$ and $M_* - Z$ relations.

4.1. AGN contamination

The traditional Baldwin-Phillips-Terlevich (BPT) diagram (Baldwin et al. 1981) can diagnose the origin of emission of narrow lines for emission-line galaxies. Figure 3 shows the locations of GRB host galaxies on the BPT diagram. The $[\text{O III}]/\text{H}\beta$ vs. $[\text{N II}]/\text{H}\alpha$ diagnostic lines are taken from Kewley et al. (2001) and Kauffmann et al. (2003). Also, the $[\text{O III}]/\text{H}\beta$ vs. $[\text{S II}]/\text{H}\alpha$ relation is from Kewley et al. (2001). This means that the GRB host galaxies are star-forming galaxies and AGN contaminations in GRB host galaxies can be ignored.

4.2. Metallicity

Metallicities of GRB hosts represented by oxygen abundance can be estimated through the T_e method and R_{23} methods. The T_e method based on electron temperature is a “direct” way. The “indirect” method is the so-called “strong-line” method, such as the R_{23} method based on the empirical relationship between O/H and R_{23} .

It has been well known that the T_e method is effective for the metal-poor galaxies because the characteristic line $[\text{O III}]\lambda 4363$ is only observable for this case. Out of 8 galaxies, 5 GRB hosts (GRB 990712, 020903, 030329, 031203, 060218) show an obvious $[\text{O III}]\lambda 4363$ line, which is a good indicator to verify that they have low metallicities and lie on the lower-metallicity branch of the R_{23} diagnostic. $[\text{N II}]/[\text{O II}]$ is also a good indicator to locate galaxy on the metallicity branch. As Kewley & Ellison (2008) suggested, the galaxies with $\log([\text{N II}]\lambda 6583/[\text{O II}]\lambda 3727) \leq -1.2$ lie on the lower metallicity branch. All those 5 objects and the GRB region of GRB 060505 have the values of $\log([\text{N II}]\lambda 6583/[\text{O II}]\lambda 3727) \leq -1.2$ while the entire GRB

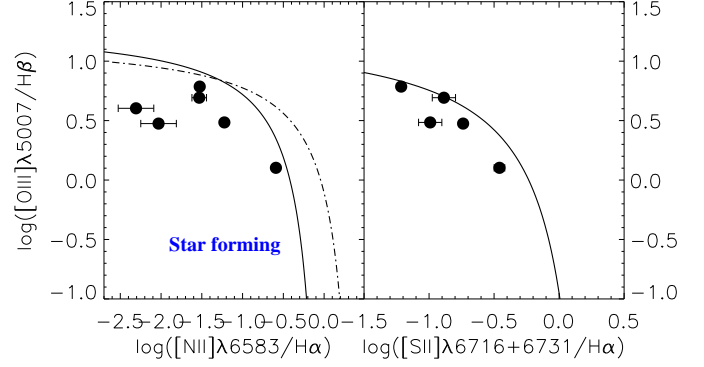


Fig. 3 The diagnostic diagrams of GRB host galaxies. In the left panel, $[\text{O III}]/\text{H}\beta$ vs. $[\text{N II}]/\text{H}\alpha$ relations is shown. The relation from Kewley et al. (2001) is drawn in the dot-dashed curve. The solid curve is from Kauffmann et al. (2003). $[\text{O III}]/\text{H}\beta$ vs. $[\text{S II}]/\text{H}\alpha$ relation from Kauffmann et al. (2003) is shown in the right panel.

060505 host galaxy lies on the upper branch, because of the value of its $\log([\text{N II}]\lambda 6583/[\text{O II}]\lambda 3727) \geq -1.2$. The values of $\log([\text{N II}]\lambda 6583/[\text{O II}]\lambda 3727)$ are given in Table 6. For another 2 GRB hosts, 980703, 020405, we can not verify which metallicity branch they lie on because their $[\text{N II}]\lambda 6583$ lines are not detected. Moreover, we use $\log([\text{N II}]\lambda 6583/\text{H}\alpha)$ to further verify the metallicity branches (≤ -1.3 for lower branch; ≥ -1.1 for upper branch, Kewley & Ellison 2008) for the sample. Those three indicators give the consistent results for those galaxies.

For the 5 host galaxies showing the $[\text{O III}]\lambda 4363$ emission line, we use the T_e method to calculate their oxygen abundances. Electron temperature and electron density are estimated using the TEMDEN task of IRAF, which is based on a 5-level atom program and was described by Shaw & Dufour (1994). The flux ratios of $[\text{O III}] I(4959 + 5007)/I(4363)$ are adopted to calculate electron temperature when available. Using the flux ratio of $[\text{S II}] I(6716)/I(6731)$, electron density can be derived, which is needed in electron temperature and oxygen abundance calculation.

When carrying out the electron density calculation, the $[\text{S II}] I(6716)/I(6731)$ doublet is not available or too noisy for some objects in our sample. Therefore we tested the sensitivities of electron temperature and oxygen abundance to electron density. The results shows that none of them is very sensitive to electron density. That allows us to estimate oxygen abundance with a wide range of electron density (20 - 200 cm^{-3}) without large bias (the discrepancy is less than 5 %).

To calculate their T_e -based oxygen abundances, we use the methods given in Stasińska (2005), Izotov et al. (2006), Yin et al. (2007), and Liang et al. (2006).

R_{23} methods have been extensively discussed in literature (Pagel et al. 1979; McGaugh 1991; Kobulnicky et al. 1999; Tremonti et al. 2004; Yin et al. 2007, and Liang et al. 2007). To estimate their R_{23} -based metallicities, we adopt the formulas from Kobulnicky et al. (1999) for both the upper and lower branches of R_{23} -(O/H) solutions. We use indicators of $[\text{N II}]\lambda 6583/[\text{O II}]\lambda 3727$ and $[\text{N II}]\lambda 6583/\text{H}\alpha$ to break the R_{23} degeneracy. The estimated oxygen abundances and errors are listed in Table 6. The T_e -based and R_{23} -based metallicity estimates have an acceptable discrepancy, 0.03-0.3dex.

Now we compare our metallicity estimates with literature. There are four objects for which their T_e -based oxygen abundances have been estimated in literature. For the host of GRB 020903, Hammer et al. (2006) give $12+\log(\text{O}/\text{H})_{T_e}$ of 7.97, which is very consistent with this work (8.01) within error-bars; Savaglio09 gave 8.22 which is 0.21 dex higher.

For the host of GRB 030329, Levesque et al. (2009) obtained 7.72 from Keck spectra, while we obtain 7.65. These two estimates are very consistent within error-bars.

For the host of GRB 031203, Prochaska et al. (2004) obtained 8.10, Margutti et al. (2007) gave 8.12, Levesque et al. (2009) obtained 7.96, and Savaglio09 gave 8.02, while we obtained 8.14. All these estimates are consistent within error-bars.

For host of GRB 060218, Wiersema et al. (2007) obtained 7.54, Levesque et al. (2009) obtained 7.62, Savaglio09 gave 7.29, and we obtained 7.88 which is closer to the second one. The discrepancy among these works could be caused by the contamination of the associated supernova. Savaglio09 gathered the very early-time spectra observed by Pian et al. (2006) and Sollerman et al. (2006). Wiersema et al. (2007) took the spectrum in 1 month after the burst, while our spectrum of the host was taken in Dec. 2006, 10 months after the burst, and Levesque et al. (2009) took the spectrum even later (19 months after the burst). In this case, the contamination of SN2006aj in the light of GRB 060218 host galaxy was significant and had lasted for several months. This contribution strongly affects measurements of emission lines; hence, the errors in the metallicity estimates from the early spectra might be large. Our result is close to the one of Levesque et al. (2009), which is also derived from the late-time observation. Anyway, all of them show this host has low metallicity.

We will not compare our R_{23} -based estimates with other work, because different calibrations give very different values, and we have discussed the discrepancy between our T_e and R_{23} -based abundances above.

4.3. Luminosity vs. metallicity

We obtain the multi-band photometry from literature, which is shown in Table 7. All apparent magnitudes are corrected for Galactic foreground extinction (Schlegel et al. 1998) and internal extinction. The k -correction is performed for the magnitudes to $z = 0$ by using the *kcorrect* v4-1-4 program⁶ (Oke & Sandage 1968; Hogg et al. 2002; Blanton & Roweis 2007). The absolute B - and K -band magnitudes corrected for Galactic extinction are given in Table 8. We plot our long-duration GRB hosts on the $L - Z$ diagram (Figure 4), which is presented in terms of absolute B magnitude and the R_{23} -based metallicities. The magnitude and metallicity of the entire GRB 060505 host galaxy are applied in the $L - Z$ diagram. For GRB 980703, the mean value between the lower and upper branch is adopted, when the R_{23} degeneracy cannot be broken. The $L - Z$ relations of various low and high redshift samples from the literature (SDSS star-forming galaxies from Tremonti et al. 2004, UV-selected galaxies from Contini et al. 2002, large magnitude-limited sample from Lamareille et al. 2004, emission-line-selected galaxies from Melbourne & Salzer 2002, irregular and spiral galaxies from Kobulnicky & Zaritsky 1999, irregular galaxies from Skillman et al. 1989 and Richer & McCall 1995) are also shown in Figure 4. In comparisons of $L - Z$ relation, the GRB hosts show an obvious discrepancy from other samples. GRB hosts have lower metallicity values compared with other galaxies at given luminosities. For luminous

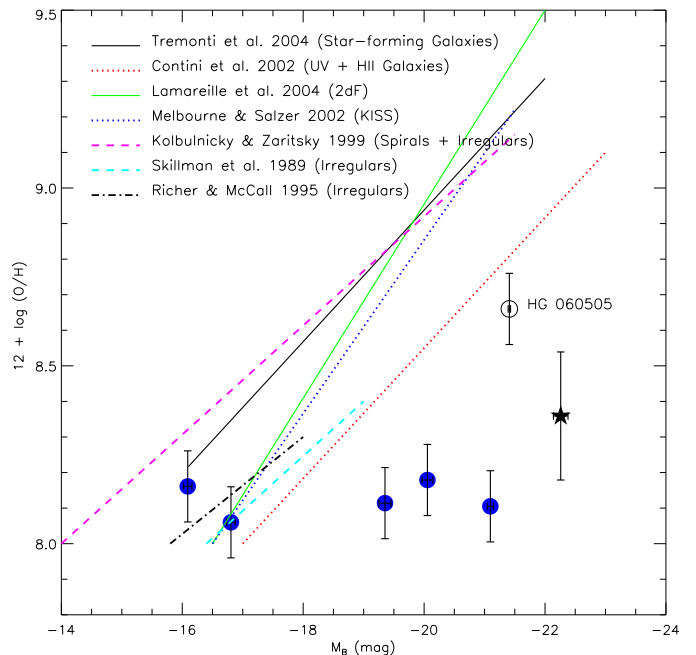


Fig. 4 The $L - Z$ relation of long-duration GRB hosts. The R_{23} -based metallicities are adopted. The blue filled circles represent oxygen abundances which break the degeneracy of R_{23} ; The black star represents the mean value between the lower and upper branch of GRB 980703. The open circle represents the entire host of GRB 060505. Luminosity-metallicity relation for SDSS galaxies and various galaxy samples are drawn from the literature (see legend). See the online color version for more details.

GRB hosts, this discrepancy is even larger. This trend is also shown in Levesque et al. (2009).

4.4. Stellar mass vs. metallicity

The stellar mass of galaxy can be estimated from the stellar mass-to-light ratio and color following Bell et al. (2003). We use the $(B - V)$ color and M_K to estimate stellar masses of GRB host galaxies. The formula is

$$\log\left(\frac{M_*}{M_\odot}\right) = -0.4(M_K - 3.28) + [a_K + b_K(B - V) + 0.15], \quad (3)$$

where M_K is the K -band absolute magnitude and $(B - V)$ is the rest-frame color. The coefficients a_K and b_K come from Table 7 on Bell et al. (2003). The stellar masses are listed in the last column of Table 8. We compare our results with previous works for GRB hosts (Chary et al. 2002, Castro Cerón et al. 2006, Castro Cerón et al. 2008, Savaglio09). Our results are more consistent with the stellar masses derived by Castro Cerón et al. (2008) within error-bars. However, our results show systematically higher values compared with their results by ~ 0.3 dex. This discrepancy between the two datasets could be caused by applying different M_*/L_K ratios. The stellar masses given by Savaglio09 are smallest among all the previous works. Castro Cerón et al. (2008) explain that the reasons for this discrepancy could be the different M_*/L_K ratios applied and the underestimated dust extinction in Savaglio09, which is also confirmed by our dust extinction (see Table 4).

⁶ <http://cosmo.nyu.edu/mb144/kcorrect/>

We plot our long-duration GRB hosts on the stellar mass-metallicity ($M_* - Z$) diagram (Figure 5). The T_e - and R_{23} -based metallicities are adopted and plotted in the left and right panels, respectively. In the right panel, the open circle and black filled star represent the entire host of GRB 060505 and GRB 980703, respectively. The $M_* - Z$ relation of local normal star-forming galaxies selected from SDSS derived by Liang et al. (2007) is given in Figure 5 (the red dashed line derived from the T_e method in the left panel; the red dotted line derived from the R_{23} method in the right panel). The T_e - and R_{23} -based metallicities of long-duration GRB host galaxies are all obviously lower than the local star-forming galaxies with comparable stellar masses.

5. Discussion and conclusion

One of the aims of this work is to find the WR presence in GRB host galaxies. According to the collapsar model, WR stars are considered as the most favored candidates of the progenitor of long-duration GRBs, therefore the presence of WR stars in long-duration GRB hosts is a direct sign to validate this model. We have investigated a sample of 8 GRB host galaxies from archival data from VLT/FORS2. Out of those 8 GRB hosts, 5 galaxies having spectra with $S/N > 10$ were chosen as a final-selected sample to detect the WR features. The presence of WR features was verified in this entire sample. Out of those 5 GRB hosts, 4 have certainly WR features detected, which are GRB 020903, GRB 031203, GRB 020405 and GRB 060218. For the remaining one, GRB 980703, the detection is marginal. The subtypes and numbers of WR stars in those 5 GRB hosts were also derived. Those results strongly support the collapsar model by revealing the link between WR stars and GRBs.

Another aim is to investigate the physical properties of long-duration GRB host galaxies, such as metallicity, luminosity and stellar mass. Comparing with literature, we used the more consistent measurements and calculation methods for all the 8 objects to ensure the systematical coherence and comparability. We found that the long-duration GRB hosts show obvious discrepancies from $L - Z$ and $M_* - Z$ relations derived in low redshift galaxies from several samples. The luminous and massive long-duration GRB hosts have lower metallicities compared with other galaxies from those samples.

The WR/O star ratio in WR galaxies is found to decrease as a function of decreasing metallicity by Crowther & Hadfield (2006). The WR/O star ratio and metallicity in GRB host galaxies do not show a clear trend. However, comparing with WR galaxies (Guseva et al. 2000), the observed WR/O ratios are higher in these GRB hosts, while metallicities in GRB hosts are obviously lower than in the numerous population of low redshift galaxies. This suggests that the hosted regions of GRBs are consistent with the first stage of star formation in a relatively pristine medium. Furthermore, the ratio of WC/WN stars is also found to decrease with metallicity. The relation between the ratio of WC/WN stars and metallicity is derived by Massey (2003). The hosts of GRB 020903, 060218 deviate from the relation, in having the higher WC/WN ratios of ~ 0.5 and 0.1 than Local Group galaxies (see their Figure 11, the upper panel). The collapsar model suggests that the WC stars are more likely to be the progenitors of long-duration GRBs rather than the WN stars. Therefore, the observed high WC/WN ratio could also be evidence to support this model, although the sample is small.

One of our galaxies, the host of GRB 060505, can be well resolved from the ground-based observation. However, the type of this burst is still a topic of hot debate. GRB 060505 has a burst duration of ~ 4 s, but lacks evidence of an accompanying super-

nova. It is classified into long-duration GRBs that have no associated supernovae (e.g. GRB 060614) by Thöne et al. (2008). However, Levesque & Kewley (2007) suggest that the environment of GRB 060505 is more consistent with the host environments of short-duration GRBs. We investigate the metallicity of the GRB site and the entire host galaxy separately. We find a relatively low metallicity in the GRB region and a higher one in the entire host. They are consistent with Thöne et al. (2008). Unfortunately, the S/N of its spectrum is not high enough to detect WR star features. However, a very young (~ 6 Myr) stellar population in the GRB site is found by Thöne et al. (2008) using stellar population modeling. This low age corresponds to the lifetime of a $32 M_\odot$ star. Evidence from the properties of the GRB region suggests that the GRB 060505 originated in a long-duration core-collapse progenitor.

Most of the GRB host galaxies in our sample are too distant to allow spatially resolved analysis with ground-based spectroscopic observations. Therefore, the information that we can have is about the global properties of galaxies. The properties of the actual explosion sites are still unclear. For further study about GRB progenitors and properties of GRB host galaxies, more high-resolution images and deep spectroscopy are needed. X-shooter at the VLT will be the ideal instrument to further investigate chemical and stellar population properties of GRBs.

Acknowledgements. We thank the anonymous referee for very helpful comments, which improve well this work. We are very grateful to H. L. Li, J. Wang, L. P. Xin, and W. K. Zheng for helpful discussions. We acknowledge James Wicker for his careful correcting of English. This work was supported by the Natural Science Foundation of China (NSFC 10933001, 10573028, 10673002, 10803008, 10821061, 10833005); the National Basic Research Program of China (973 Program, 2007CB815402, 2007CB815404, 2007CB815406, 2009CB824800); the Young Researcher Grant of National Astronomical Observatories, Chinese Academy of Sciences; and the Group Innovation Project (10821302). The STARLIGHT project is supported by the Brazilian agencies CNPq, CAPES and FAPESP and by the France-Brizil CAPES/Cofecub program.

References

- Allen, D. A., Wright, A. E., & Goss, W. M. 1976, MNRAS, 177, 91
- Arnault, Ph., Kunth, D., & Schild, H. 1989, A&A, 224, 73
- Baldwin, A., Phillips, M. M., & Terlevich, R. 1981, PASP, 93, 817
- Barlow, M. J., & Hummer, D. G. 1982, in IAU Symp. 99, Wolf-Rayet Stars: Observations, Physics, and Evolution, ed. C. W. H. de Loore & A. J. Willis (Dordrecht: Reidel), 387
- Bell, E. F., McIntosh, D. H., Katz, N., Weinberg, M. D. 2003, ApJS, 149, 289
- Berger, E. 2008, e-prints, arXiv:0805.0306v1
- Bersier, D., Fruchter, A. S., Strolger, L. G., et al. 2006, ApJ, 643, 284
- Blanton, M. R., & Roweis, S. 2007, AJ, 133, 734
- Brinchmann, J., Kunth, D., & Durret, F. 2008, A&A, 485, 657
- Bruzual, G., & Charlot, S. 2003, MNRAS, 344, 1000
- Cardelli, J. A., Clayton, G. C., & Mathis, J. S. 1989, ApJ, 345, 245
- Castro Cerón, J. M., Michalowski, M. J., Hjorth, J. et al. 2006, ApJ, 653, 85
- Castro Cerón, J. M., Michalowski, M. J., Hjorth, J. et al. 2008, e-prints, arXiv:0803.2235v2
- Chary, R., Becklin, E. E., & Armus, L. 2002, ApJ, 566, 229
- Christensen, L., Hjorth, J., & Gorosabel, J. 2004, A&A, 425, 913
- Cid Fernandes, R., Mateus, A., Sodré, L., Stasińska, G., Gomes, J. M. 2005, MNRAS, 358, 363
- Conti, P. S. 1991, ApJ, 377, 115
- Conti, P. S., Leep, E. M., & Perry, D. N. 1983, ApJ, 268, 228
- Contini, T., Treyer, M. A., Sullivan, M., & Ellis, R. S. 2002, MNRAS, 330, 75
- Courty, S., Björnsson, G., & Gudmundsson, E. H. 2004, MNRAS, 354, 581
- Crowther, P. A., & Hadfield, L. J. 2006, A&A, 449, 711
- Crowther, P. A., & Smith, L. J. 1997, A&A, 320, 500
- Dinerstein, H. L., & Shields, G. A., 1986, ApJ, 311, 45
- Fynbo, J. P. U., Jakobsson, P., Möller, P., et al. 2003, A&A, 406, L63
- Fynbo, J. P. U., Watson, D., Thöne, C. C., et al. 2006, Nature, 444, 1047
- Gorosabel, J., Jelińek, M., de Ugarte Postigo, A., Guziy, S., & Castro-Tirado, A. J., 2005, Nuovo Cimento C, 28, 677
- Guseva, N. G., Izotov, Y. I., & Thuan, T. X. 2000, ApJ, 531, 776

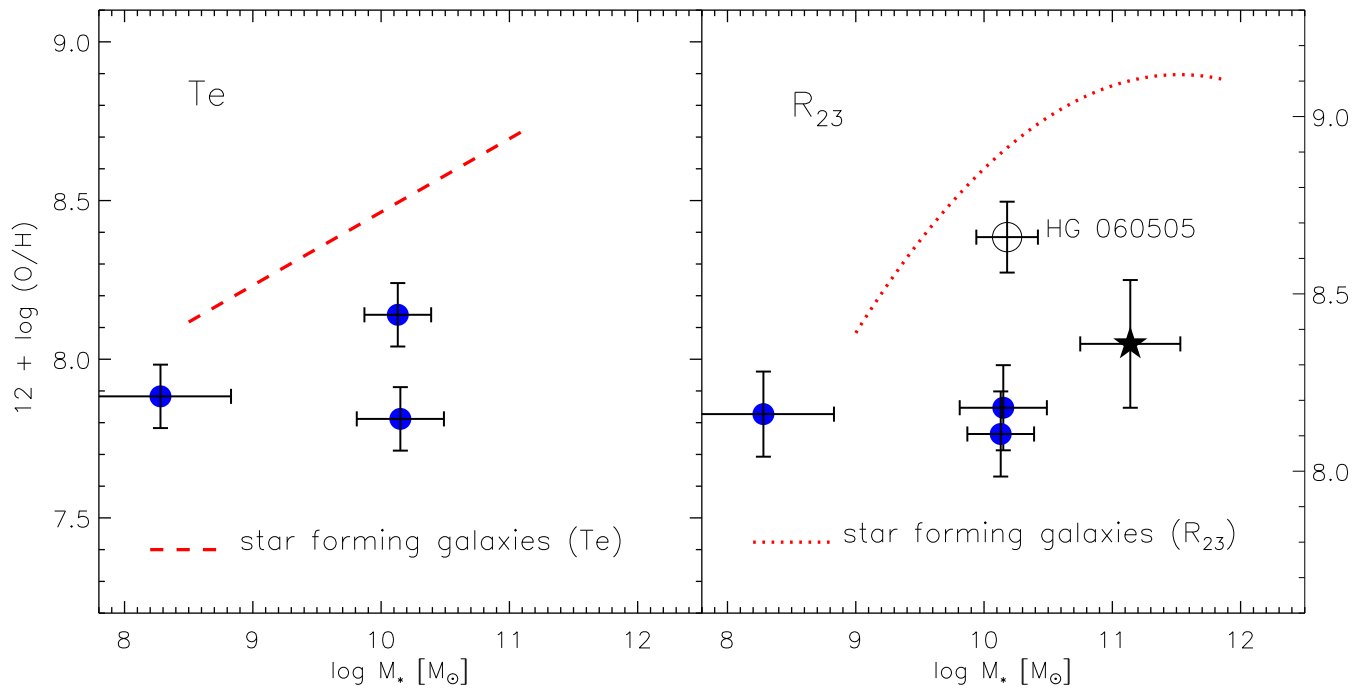


Fig. 5 In the left panel, the T_e -based (the filled circles) oxygen abundances of long-duration GRB hosts are given. The red dashed line refers to the M_* – Z relation of local star-forming galaxies from SDSS derived from T_e method (Liang et al. 2007). In the right panel, we plot the R_{23} -based oxygen abundances of long-duration GRB hosts derived using the formulas from Kobulnicky et al. (1999, K99) (the blue filled circles - oxygen abundances which break the degeneracy; the black star - oxygen abundances from mean value between the lower and upper branch). The open circle represents the entire host of GRB 060505. The red dotted line refers to the M_* – Z relation of local star-forming galaxies from SDSS derived from R_{23} method (Liang et al. 2007). See the online color version for more details.

- Hammer, F., Flores, H., Schaerer, D., Dessauges-Zavadsky, M. Le Floc'h, E., & Puech, M. 2006, *A&A*, 454, 103
 Hartmann, D. H. 2005, *Nature*, 436, 923
 Hirschi, R., Meynet, G., & Maeder, A. 2005, *A&A*, 443, 581
 Hjorth, J., Watson, D., Fynbo, J. P. U., et al. 2005, *Nature*, 437, 859
 Hogg, D. W., Blanton, M., Strateva, I., et al. 2002, *AJ*, 124, 646
 Izotov, Y. I., Stasińska, G., Meynet, G., Guseva, N. G., Thuan, T. X. 2006, *A&A*, 448, 955
 Izotov, Y. I., & Thuan, T. X. 1998, *ApJ*, 500, 188
 Kauffmann, G., Heckman, T. M., Tremonti, C., et al. 2003, *MNRAS*, 346, 1055
 Kewley, L. J., Brown, W. R., Geller, M. J., Kenyon, S. J., & Kurtz, M. J. 2007, *AJ*, 133, 882
 Kewley, L. J., Dopita, M. A., Sutherland, R. S., Heisler, C. A., Trevena, J. 2001, *ApJ*, 556, 121
 Kewley, L. J., & Ellison, S. L. 2008, *ApJ*, 681, 1183
 Klebesadel, R. W., Strong, I. B., & Olson, R. A. 1973, *ApJ*, 182, 85
 Klose, S., Greiner, J., Rau, A., et al. 2004, *AJ*, 128, 1942
 Kobulnicky, H. A., Kennicutt, R. C. Jr., & Pizagno, J. L. 1999, *ApJ*, 514, 544
 Kobulnicky, H. A. & Zaritsky, D. 1999, *ApJ*, 511, 118
 Kocevski, D., Modjaz, M., Bloom, J. S., et al. 2007, *ApJ*, 663, 1180
 Kouveliotou, C., Meegan, C. A., Fishman, G. J., et al. 1993, *ApJ*, 413, 101
 Kunth, D., & Joubert, M. 1985, *A&A*, 142, 411
 Kunth, D., & Schild, H. 1986, *A&A*, 169, 71
 Lamareille, F., Mouhcine, M., Contini, T., Lewis, L., & Maddox, S. 2004, *MNRAS*, 350, 396
 Le Floc'h, E., Duc, P. -A., Mirabel, I. F., et al. 2003, *A&A*, 400, 499
 Levesque, E. M., & Kewley, L. J. 2007, *ApJ*, 667, 121
 Levesque, E. M., Berger, E., Kewley, L. J., & Bagley, M. M. 2009, e-points, arXiv:0907.4988v3
 Liang, Y. C., Hammer, F., Deng, L. C., & Zhao, G. 2006, *PABei*, 24, 335
 Liang, Y. C., Hammer, F., Yin, S. Y., Flores, H., Rodrigues, M., Yang, Y. B. 2007, *A&A*, 473, 411
 MacFadyen, A. I., & Woosley, S. E. 1999, *ApJ*, 524, 262
 Margutti, R., Chincarini, G., Covino, S., et al. 2007, *A&A*, 474, 815
 Massey, P., 2003, *ARA&A*, 41, 15
 Massey, P., & Conti, P. 1980, *ApJ*, 242, 638
 Massey, P., & Conti, P. 1983, *PASP*, 95, 440
 McGaugh, S. S. 1991, *ApJ*, 380, 140
 Melbourne, J., & Salzer, J. J. 2002, *AJ*, 123, 2302
 Oke, J. B., & Sandage, A. 1968, *ApJ*, 154, 21
 Osterbrock, D. E. 1989, *Astrophysics of Gaseous Nebulae and Active Galactic Nuclei* (Mill Valley, California: University Science Books)
 Pagel, B. E., Edmunds, M. G., Blackwell, D. E., Chun, M. S., Smith, G. 1979, *MNRAS*, 189, 95
 Petrovic, J., Langer, N., Yoon, S. -C., Heger, A. 2005, *A&A*, 435, 247
 Pian, E., Mazzali, P. A., Masetti, N., et al. 2006, *Nature*, 442, 1011
 Prochaska, J. X., Bloom, J. S., Chen, H. -W., et al. 2004, *ApJ*, 611, 200
 Richer, M. G., & McCall, M. L., 1995, *ApJ*, 445, 642
 Salpeter, E. E. 1955, *ApJ*, 121, 161
 Savaglio, S., Glazebrook, K., & Le Borgne, D. 2009, *ApJ*, 691, 182
 Schaerer, D., & Vacca, W. D., 1998, *ApJ*, 497, 618
 Schlegel, D. J., Finkbeiner, D. P., & Davis, M. 1998, *ApJ*, 500, 525
 Seaton, M. J. 1979, *MNRAS*, 187, 73
 Shaw, R. A., & Dufour, R. J. 1994, *Astronomical Data Analysis Software and Systems III*, ed. D. R. Crabtree, R. J. Hanisch, & J. Barnes, ASP Conf. Ser., 61, 327
 Skillman, E. D., Kennicutt, R. C., Jr., & Hodge, P. W. 1989, *ApJ*, 347, 875
 Smith, L. F., Shara, M. M., & Moffat, A. F. G., 1996, *MNRAS*, 281, 163
 Soderberg, A. M., Kulkarni, S. R., Berger, E., 2004, *ApJ*, 606, 994
 Sokolov, V. V., Fatkhullin, T. A., Castro-Tirado, A. J., et al. 2001, *A&A*, 372, 438
 Sollerman, J., Jaunsen, A. O., Fynbo, J. P. U., et al. 2006, *A&A*, 454, 503
 Stasińska, G. 2005, *A&A*, 434, 507
 Thöne, C. C., Fynbo, J. P. U., Östlin, G., et al. 2008, *ApJ*, 676, 1151
 Tremonti, C. A., Heckman, T. M., Kauffmann, G. et al. 2004, *ApJ*, 613, 898
 Torres, A. V., Conti, P. S., & Massey, P. 1986, *ApJ*, 300, 379
 Vacca, W. D., & Conti, P. S. 1992, *ApJ*, 401, 543
 van der Hucht, K. A., Conti, P. S., Lundström, I., & Stenholm, B. 1981, *Space Sci. Rev.*, 28, 227
 van Paradijs, J., Groot, P. J., Galama, T., et al. 1997, *Nature*, 386, 686
 Vreeswijk, P. M., Galama, T. J., Owens, A., et al. 1999, *ApJ*, 523, 171
 Wainwright, C., Berger, E., & Penprase, B. E. 2007, *ApJ*, 657, 367
 Wiersema, K., Savaglio, S., Vreeswijk, P. M., et al. 2007, *A&A*, 464, 529
 Woosley, S. E., Langer, N., & Weaver, T. A. 1993, *ApJ*, 411, 823
 Woosley, S. E., & Heger, A. 2006, *ApJ*, 637, 914

- Yin, S. Y., Liang Y. C., Hammer, F., Brinchmann, J., Zhang, B., Deng, L. C.,
Flores, H. 2007, A&A, 462, 535
Yoon, S. -C., & Langer, N. 2005, A&A, 443, 643

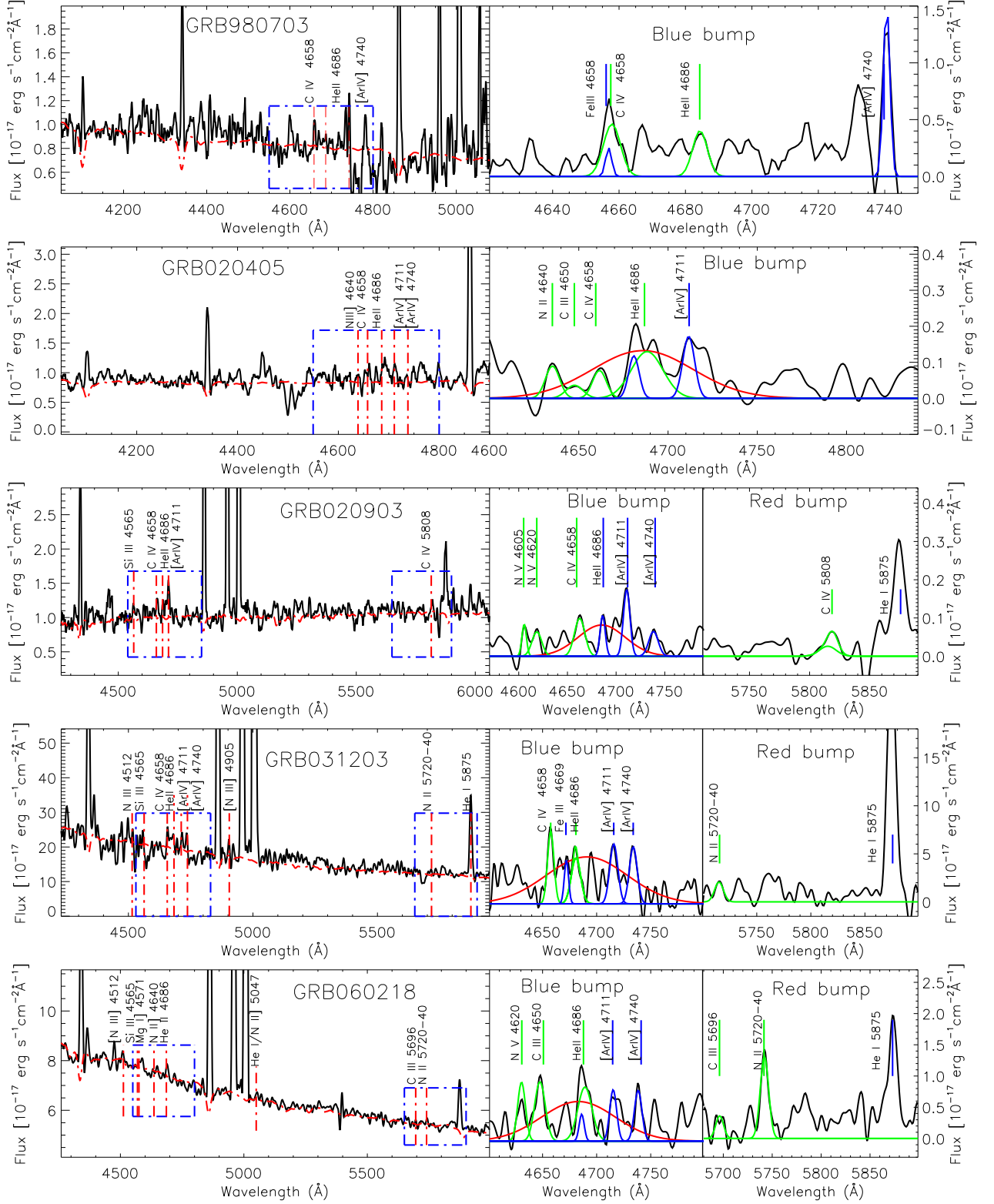


Fig. 2 The spectra of GRB hosts are plotted in the left panels. The continuums are marked using red lines, which are the results of the Starlight fit using BC03 templates. The blue boxes indicate the WR blue and red bumps. The WR emission lines are marked in red dot-dashed lines. In the right panels, the fits of WR bumps are plotted in red profiles. The fits of individual WR line and nebular line are plotted in green and blue profiles respectively (for more details, please see the online color version.)

Table 1 Basic information of the GRB host galaxies

GRB	RA ^a	DEC ^a	z	E _G (B - V) ^b	Type
GRB 980703	23 : 59 : 07	08 : 33 : 36	0.966	0.061	long
GRB 990712	22 : 31 : 50	-73 : 24 : 29	0.433	0.033	long
GRB 020405	13 : 58 : 03	-31 : 22 : 22	0.691	0.055	long
GRB 020903	22 : 49 : 25	-20 : 53 : 59	0.251	0.033	long
GRB 030329	10 : 44 : 50	21 : 31 : 17	0.168	0.025	long
GRB 031203	08 : 02 : 28	-39 : 51 : 04	0.105	1.040	long
GRB 060218	03 : 21 : 39	16 : 52 : 02	0.034	0.140	long
GRB 060505	22 : 07 : 01	-27 : 48 : 56	0.089	0.021	long?

Notes: (a) Coordinates at the 2000.0 epoch. (b) Galactic extinction (Schlegel et al. 1998)

Table 2 Spectroscopic observations of GRB host galaxies from VLT/FORS2

UT Date	Exposure time(second)	seeing ^a (")	Grism	Program ID
GRB980703				
2004.07.15 - 17	8 × 1200	0.75	600Z	073.B - 0482(A)
2004.07.16 - 17	8 × 1200	0.75	600RI	073.B - 0482(A)
GRB990712				
2005.07.05 - 06	4 × 1800	0.59	300V	075.D - 0771(A)
GRB020405				
2004.07.15 - 16	9 × 1200	0.70	600RI	073.B - 0482(A)
GRB020903				
2004.07.15	6 × 1200	0.55	600B	073.B - 0482(A)
2004.07.16	6 × 1200	0.83	600RI	073.B - 0482(A)
GRB030329				
2003.04.10	6 × 600	1.18	300V	071.D - 0355(B)
2003.04.17	2 × 300	0.71	300V	071.D - 0355(B)
2003.04.22	1 × 300	0.71	300V	071.D - 0355(B)
2003.05.01	2 × 600	0.51	300V	071.D - 0355(B)
2003.06.19	3 × 900	0.75	300V	271.D - 5006(A)
GRB031203				
2003.12.20	2 × 2700	0.50	300V	072.D - 0480(A)
2004.09.20	2 × 1800	0.60	300V	073.D - 0255(A)
2005.03.28	4 × 1200	0.69	300V	073.D - 0418(A)
2005.04.09	3 × 1200	1.26	300V	075.D - 0771(A)
GRB060218				
2006.11.27	1 × 3100	0.97	300V	078.D - 0246(A)
2006.12.19 - 20	3 × 3150	0.72	300V	078.D - 0246(A)
GRB060505				
2006.05.23	2 × 1800 + 1327 + 600	0.81	300V	077.D - 0661(B)

Notes: (a) Seeing is the average value in the observing night.

Table 3 Emission line fluxes of GRB host galaxies (in units of 10^{-17} erg s $^{-1}$ cm $^{-2}$, corrected for Galactic extinction)

Ion	980703	990712	020405	020903	030329	031203	060218	060505 ^a	060505 ^b
[OII] λ 3727	24.28 \pm 0.11	23.26 \pm 0.15	11.53 \pm 0.16	11.48 \pm 0.36	19.62 \pm 0.32	943.07 \pm 4.80	224.25 \pm 1.01	20.96 \pm 0.82	50.33 \pm 1.88
H δ	1.66 \pm 0.22	1.95 \pm 0.09	–	1.76 \pm 0.24	–	204.83 \pm 4.41	20.11 \pm 0.57	–	–
H γ	3.1 \pm 0.19	4.9 \pm 0.10	1.9 \pm 0.09	3.94 \pm 0.29	4.41 \pm 0.10	499.73 \pm 1.10	42.02 \pm 0.67	3.79 \pm 0.30	–
[OIII] λ 4363	–	0.92 \pm 0.08	–	0.55 \pm 0.07	0.71 \pm 0.05	79.10 \pm 1.25	4.77 \pm 0.30	–	–
[FeIII] λ 4658	0.16 \pm 0.09	–	–	–	–	–	–	–	–
HeII λ 4686	–	–	0.05 \pm 0.03	0.39 \pm 0.06	–	1.20 \pm 0.92	0.81 \pm 0.31	–	–
[ArIV] λ 4711	–	–	0.07 \pm 0.10	0.80 \pm 0.25	–	4.90 \pm 3.11	2.12 \pm 0.84	–	–
[ArIV] λ 4740	1.01 \pm 0.05	–	–	0.41 \pm 0.10	–	3.81 \pm 2.91	2.28 \pm 0.91	–	–
H β	6.79 \pm 0.30	11.29 \pm 0.07	5.36 \pm 0.10	8.58 \pm 0.29	9.80 \pm 0.16	1135.37 \pm 5.21	91.43 \pm 0.65	8.90 \pm 0.32	21.02 \pm 0.51
[OIII] λ 4959	4.51 \pm 0.41	17.37 \pm 0.11	5.19 \pm 0.06	15.56 \pm 0.31	11.74 \pm 0.20	2404.78 \pm 5.32	108.4 \pm 0.48	8.47 \pm 0.24	12.47 \pm 0.32
[OIII] λ 5007	14.39 \pm 0.33	47.28 \pm 0.09	18.33 \pm 0.13	44.11 \pm 0.33	30.53 \pm 0.26	7238.76 \pm 4.68	291.23 \pm 0.66	20.48 \pm 0.48	27.80 \pm 2.30
H α	–	40.34 \pm 0.32	–	26.03 \pm 0.21	30.94 \pm 0.27	3636.63 \pm 4.96	261.51 \pm 0.54	31.49 \pm 0.44	114.8 \pm 3.66
[NII] λ 6583	–	< 0.41 \pm 0.20	–	0.77 \pm 0.10	0.29 \pm 0.15	109.04 \pm 4.21	10.73 \pm 0.32	1.79 \pm 0.09	29.62 \pm 0.29
[SII] λ 6716	–	–	–	2.14 \pm 0.17	3.82 \pm 0.09	129.55 \pm 4.33	15.4 \pm 0.36	3.46 \pm 0.13	26.36 \pm 0.51
[SII] λ 6731	–	–	–	1.28 \pm 0.09	1.89 \pm 0.08	94.63 \pm 2.89	11.56 \pm 0.41	2.80 \pm 0.20	13.98 \pm 0.19

Notes: (a) GRB site. (b) The entire host galaxy.

Table 4 Dust extinction of GRB host galaxies

GRB	H α /H β	H γ /H β	A $_V$ (H α /H β)	A $_V$ (H γ /H β)	E $_{\text{HG}}$ (B – V)
980703	–	0.46 \pm 0.23	–	0.14 \pm 0.53	0.05 \pm 0.17
990712	3.57 \pm 0.41	0.43 \pm 0.11	0.55 \pm 0.03	0.50 \pm 0.15	0.18 \pm 0.01
020405	–	0.35 \pm 0.10	–	1.93 \pm 0.36	0.62 \pm 0.12
020903	3.03 \pm 0.91	0.46 \pm 0.32	0.15 \pm 0.09	0.10 \pm 0.57	0.05 \pm 0.03
030329	3.16 \pm 0.57	0.45 \pm 0.12	0.24 \pm 0.05	0.25 \pm 0.20	0.08 \pm 0.02
031203	3.20 \pm 1.79	0.44 \pm 0.25	0.28 \pm 0.04	0.40 \pm 0.12	0.09 \pm 0.01
060218	2.86 \pm 1.64	0.46 \pm 0.34	0.00 \pm 0.02	0.10 \pm 0.12	0.00 \pm 0.01
060505 ^a	3.54 \pm 3.59	0.43 \pm 0.72	0.53 \pm 0.08	0.63 \pm 0.35	0.17 \pm 0.03
060505 ^b	5.46 \pm 4.51	–	1.60 \pm 0.31	–	0.52 \pm 0.10

Notes: (a) GRB site. (b) The entire host galaxy.

Table 5 Properties of WR stars in GRB hosts

Ion	980703		020405		020903		031203		060218	
	<i>F</i>	<i>L</i>	<i>F</i>	<i>L</i>	<i>F</i>	<i>L</i>	<i>F</i>	<i>L</i>	<i>F</i>	<i>L</i>
blue bump ($\lambda 4650$) ^a	-	-	0.18±0.09	654.39±326.21	1.52±0.31	97.22±42.90	10.65±6.06	114.87±65.37	8.08±3.25	6.49±2.41
red bump ($\lambda 5008$)	-	-	-	-	0.50±0.10	32.10±7.30	-	-	-	-
CIII $\lambda 5696$	-	-	-	-	-	-	-	-	3.76±1.10	2.48±0.76
WNL	-	-	-	-	2117±721	-	5743±3268	-	324±120	-
WCE	-	-	-	-	1070±210	-	-	-	-	-
WCL	-	-	-	-	-	-	-	-	31±10	-
WR/O	-	-	0.04±0.03	-	0.21±0.06	-	0.01±0.01	-	0.11±0.04	-

Notes: WR emission line fluxes (*F*, corrected for Galactic extinction) are in units of 10^{-17} erg s⁻¹ cm⁻², Luminosities (*L*) are in units of 10^{38} erg s⁻¹.

(a) Fluxes and luminosities of nebular lines were subtracted.

Table 6. Metallicities of GRB host galaxies

	980703	990712	020405	020903	030329	031203	060218	060505 ^g	060505 ^h
N _e [SII] ^a	-	20 ~ 200	-	20 ~ 200	20 ~ 200	52.63 ± 43.20	120.68 ± 32.22	-	-
T _e [OIII] ^b	-	16434.9 ± 425.8	-	13517.1 ± 335.2	17911.7 ± 325.0	12902.2 ± 305.2	15113.3 ± 335.5	-	-
12 + log (O/H)(Te) ^c	-	7.812 ± 0.15	-	8.014 ± 0.15	7.653 ± 0.14	8.142 ± 0.07	7.883 ± 0.09	-	-
12 + log (O/H)(K99 _L) ^d	8.28 ± 0.14	8.18 ± 0.12 ^f	8.10 ± 0.12	8.11 ± 0.12 ^f	8.06 ± 0.10 ^f	8.11 ± 0.11 ^f	8.16 ± 0.14 ^f	8.06 ± 0.14 ^f	7.99 ± 0.09
12 + log (O/H)(K99 _U) ^d	8.44 ± 0.15	8.47 ± 0.15	8.53 ± 0.15	8.50 ± 0.15	8.56 ± 0.16	8.51 ± 0.15	8.50 ± 0.16	8.57 ± 0.15	8.66 ± 0.16 ^f
log ([NII]6583/[OII]3727)	-	-2.36	-	-1.47	-2.12	-1.23	-1.45	-1.36	-0.52
A _V ^e	0.144 ± 0.532	0.551 ± 0.025	1.927 ± 0.359	0.146 ± 0.086	0.244 ± 0.046	0.280 ± 0.040	0.000 ± 0.018	0.526 ± 0.081	1.601 ± 0.310

^aElectronic density estimated from the [S II] flux ratio: $I(6716)/I(6731)$.

^bTemperature in K estimated from the following flux ratios: [O III] $I(4959 + 5007)/I(4363)$

^cMetallicity, 12+log(O/H), estimated using the effective temperature method.

^dMetallicity, 12+log(O/H), estimated following Kobulnicky et al. 1999 (K99). K99_L (their Equation 8) is valid for the lower branch; K99_U (their Equation 9) is valid for the upper branch.

^eExtinction coefficient, A_V (in magnitude) is derived using the standard Balmer ratio of H α and H β . For GRB 980703 and 020405, A_V from the ratio of H γ and H β is adopted.

^fAdopted metallicity in this work. The R_{23} degeneracy are broken using the [N II]/H α and [N II]/[O II] ratios.

^gThe GRB site

^hThe entire host galaxy

Table 7. Photometry of GRB host galaxies

GRB	U	B	V	R	I	J	H	K	<i>Refs</i>
980703	-	23.40±0.12	23.04±0.08	22.58±0.06	21.95±0.25	20.87±0.11	20.27±0.19	19.62±0.12	1, 2, 3
990712	23.12±0.05	23.36±0.09	22.39±0.03	21.84±0.02	21.41±0.03	20.81±0.17	20.25±0.19	20.05±0.10	3
020903	-	21.70±0.10	20.80±0.10	20.80±0.10	20.50±0.10	-	-	-	4, 5
030329	22.68±0.10	23.42±0.07	22.88±0.05	22.80±0.04	-	21.52±0.04	21.17±0.24	-	6
031203	22.41±0.18	22.32±0.05	20.53±0.05	20.44±0.02	19.40±0.04	18.28±0.02	17.78±0.02	16.54±0.02	7
060218	20.45±0.15	20.46±0.07	20.19±0.04	19.86±0.03	19.47±0.06	18.99±0.16	18.52±0.22	18.69±0.34	8, 9, 10
060505	18.43±0.05	18.89±0.02	18.27±0.02	17.90±0.02	17.51±0.02	17.29±0.08 ^a	-	15.85±0.04	11
020405	-	-	F555W ^b	F702W ^b	F814W ^b	-	-	-	12
	-	-	22.63±0.05	21.84±0.05	21.29±0.05	-	-	-	

Note. — references: (1) Vreeswijk et al. 1999; (2) Sokolov et al. 2001; (3) Christensen et al. 2004; (4) Soderberg et al. 2004; (5) Bersier et al. 2006; (6) Gorosabel et al. 2005; (7) Margutti et al. 2007; (8) Sollerman et al. 2006; (9) Castro Cerón et al. 2008; (10) Kocevski et al. 2007; (11) Thöne et al. 2008; (12) Wainwright et al. 2007

Note. — The magnitudes are not corrected for Galactic extinction.

^aFORS1 z filter (Central wavelength: 9100 Å; Band width: 1305 Å).

^bF555W (Central wavelength: 5407 Å; Band width: 1236 Å); F702W (Central wavelength: 6895 Å; Band width: 1389 Å); F814W (Central wavelength: 7940 Å; Band width: 1531 Å)

Table 8. Magnitudes and stellar masses of GRB host galaxies

GRB	M_B	M_K	$\log M_* [M_\odot]$
980703	-20.85 ± 0.12	-24.41 ± 0.12	11.14 ± 0.39
990712	-18.67 ± 0.09	-21.85 ± 0.10	10.14 ± 0.34
020405	-	-	-
020903	-18.96 ± 0.10	-	-
030329	-16.22 ± 0.07	-	-
031203	-20.58 ± 0.05	-22.27 ± 0.02	10.13 ± 0.26
060218	-16.02 ± 0.07	-17.23 ± 0.34	8.28 ± 0.55
060505 ^a	-19.24 ± 0.02	-22.20 ± 0.04	10.18 ± 0.24

Note. — Absolute magnitudes M_B and M_K are corrected for galactic foreground extinction (Schlegel et al. 1998).

^aThe magnitudes and stellar mass of the entire galaxy of GRB 060505 host